Optimization of the Compensation Networks for WPT Systems

Manuele Bertoluzzo, Mattia Forato, *Student Member, IEEE*, and Elisabetta Sieni
Department of Industrial Engineering, University of Padova, Padova, Italy
manuele.bertoluzzo@unipd.it, mattia.forato@studenti.unipd.it, elisabetta.sieni@unipd.it

***Abstract* –Performance of wireless power transfer systems are greatly influenced by the topology and the sizing of the compensation networks connected to the coils and number of design procedures have been proposed to optimize one or the other characteristic of the system acting on their parameters. This paper introduces a method base on an optimization algorithm to design the compensation networks with the objective of optimizing the power transfer efficiency and the amount of transferred power for a given supply voltage amplitude. The soundness of the method has been checked comparing the obtained results with those achieved analytically in the case of the simple SS compensation topology, and checking by means of amplitude Bode diagrams the outcomes relevant to more complex topologies.**

Index Terms— Inductive power transfer, compensation networks, optimization.

I. INTRODUCTION

Wireless power transfer is a promising technology that will make the charging of electric vehicles easier and more user friendly, overcoming the prejudices of many people against tampering with electric devices [1], [2]. One of the main components of the wireless power transfer systems (WPTSs) are the compensation networks (CNs) connected to the coupled coils. They are ideally composed by purely reactive elements and have been initially introduced to increase the power transfer efficiency and to contain the sizing power of the static converters and of the coils themselves; nowadays they are also in charge of tuning a number of characteristics of the WPTSs to the particular application, especially if dynamic WPTSs are considered [3], [4].

Different topologies have been proposed for the CNs, sometimes including several elements and requiring rather involved sizing procedures aimed at improving the performance of the systems. Most of these procedures work out the reactance of the CNs' elements using an analytical approach, but sometimes arbitrary design choices are taken. At the moment, a definite method to select the topology of the CNs and to size their elements on the basis of WPTS specifications is not available. In most of the cases the elements sizing is based on the study of the WPTS circuital equations to work out the relations between the reactances of the CNs elements and the system characteristics. The subsequent inversion of these relations allows to compute the elements reactance as a function of the system specifications. This last operation is rather difficult so that additional simplifying hypotheses are often introduced to reach a result.

Often in electrical engineering the design problems are tackled using the optimization approach, formulating them as bi-objective or many-objective ones [5]–[9]; a typical example is the shape design of electromagnetic devices that often requires that multiple criteria are satisfied simultaneously [6], [10]–[16]. This is true also in circuit design, where the parameters of the electric and/or electronic components have to be determined in order to obtain a given performance of the circuit.

This paper proposes to apply this approach to the sizing of the CNs of WPTS. Being the CNs reactances adjusted by an iterative process, the inversion of the relations between the CNs reactance and the WPTS characteristics is not needed and it is possible to investigate the possibilities offered by the CNs without simplifying hypotheses or limitations in the explored ranges of the CNs reactances. In this way, complex CNs can be studied without the limitation arising from the computation complexity inherent in the circuital analysis of RLC networks. Moreover, this approach can be applied also to CNs with conventional topology, such as SS, SP, PS and PP, to study their performance when resonating conditions different from those usually considered are enforced.

In this paper, two different examples of CNs have been selected as test bench for the optimization algorithm: the first has the SS topology, whilst the second is much more complex and exhibits a T topology both at the transmitter and the receiver side. For both of them two operating condition have been considered in order to test the ability of the algorithm of generating satisfactory results in a wide range of different applications. More in detail, this paper describes an optimization method based on the Non-dominated Sorting Genetic Algorithm (NSGA-II) [9], which showed good results in different fields of application, e.g. in MEMS synthesis [17], [18], induction heating applications [19] and bioelectromagnetics [20].

The paper is organized as follows. Section II reviews briefly the architecture and the functioning of WPTSs and illustrates the specification to be satisfied by the CNs. Section III describes the optimization method and how its objective functions are developed. In Section IV the optimization method is checked comparing its results with those obtained analytically when optimization of CNs with series-series (SS) topology is performed. Section V reports the results obtained considering CNs having more complex topology. Section VI validates the assumptions made in developing the objective functions and the obtained results. Section VII concludes the paper.

II. WPTS FUNCTIONING

Functioning of WPTSs is based on the inductive coupling between a coil, usually named pickup, installed onboard the vehicle and a transmitting coil, deployed under the road surface and over which the vehicle is parked during the charging. The transmitting coil is supplied by a high frequency inverter and

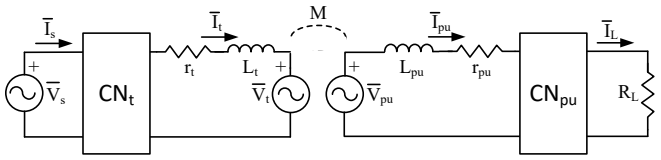

Figure 1. Equivalent circuit of a WPTS considering the coupling between the pickup and the transmitting coil.

induces a voltage across the terminal of the pickup whenever they are coupled. The induced voltage is suitably conditioned by a rectifier to supply the dc bus of the vehicle from which the battery charger draw the required power.

Figure 1 reports the equivalent circuit usually adopted to study the WPTSs. It considers a transmitting coil coupled to the pickup by a mutual inductance M. The transmitting coil and the pickup have self-inductances L_t and L_{pu} and are connected to the CNs represented by the blocks CN_t and CN_{pu}. Usually CNs are tuned to resonate at the supply frequency and effectively attenuate the higher order current harmonics. Hence, the active power transferred to the load depends only on the first harmonic components of the electric quantities involved in the functioning of the system while the others, in a first approximation, can be disregarded. For this reason, the phasor notation is used for the voltages and the currents in Figure 1. In particular, $\bar{V}_t$ and $\bar{V}_{pu}$ are the voltages induced across the coils terminals respectively by the currents $\bar{I}_{pu}$ and $\bar{I}_t$, $\bar{V}_s$ is the first harmonic of the voltage $v_s(t)$ generated by the high frequency inverter, which usually has a square waveform, and $\bar{I}_s$ is the supply current. The power converter at the pickup side of the WPTS and the equivalent load constituted by the battery are represented by an equivalent load resistance R_L supplied by the current $\bar{I}_L$. Resistances r_t and r_{pu} are the equivalent series resistances of the coils and cause most of the losses in the WPTS; sometimes, in studying the system, their values are adjusted in order to account also for the losses in the power converters and in the CNs.

The main requirements of a WPTS is to transfer enough power to charge the battery with an efficiency as high as possible. Moreover, the sizing power of the system should not exceed too much the power required to charge the battery, in order to avoid oversizing the WPTS components, with a consequent increase of its cost, weight and volume.

These requirements can be summarized in the two objective of maximizing the power transfer efficiency and the amount of transmitted power per unity of supply voltage amplitude. The first objective is obviously equivalent to the first requirement, and, being the losses concentrated in r_t and r_{pu}, it entails transferring the required power with minimum currents in the coils. The second objective requires to increase the currents in the coils to maximize the power with a given voltage, and consequently is in contrast with the first one. From this consideration it derives that this approach to the CNs design falls in the class of the bi-objective problems.

III. Optimization Method

The optimization method operates starting from the design variables that appear in the equations that describe the behavior of the WPTS with the aim of searching for the maximum of two objective function derived from the WPTS objectives. As explained in the previous Section, the objective functions for this application are in contrast so that a Pareto front of non-dominated solutions is obtained.

A. NSGA-II Algorithm

The NSGA-II algorithm starts processing a number of sets of design variables; each set is defined as an individual and all together they form the initial population. The design variables are the reactances of the elements of the CNs, and, depending on the considered topology, there are two or six variables in each individual. The initial population is generated extracting the individuals from a uniform distribution defined in the range $[B_{min}, B_{max}]$. In this case, the boundaries of this interval have been set to one order of magnitude higher than the reactance of the coils, allowing the design variables to take both positive and negative values.

Each successive generation is obtained applying the genetic operator to the individuals of the previous one: from a number of pairs of individuals, one or two sons are generated using the genetic rules of cross over, as described in [21]; then the individuals that best fit with a given selection criterion, expressed by means of the objective functions, are selected to constitute the new generation. After a fixed number of generations the algorithm is stopped.

B. Objective functions

The optimization algorithm selects the most suited individuals among those that maximize a pair of objective functions. The functions depend on the design variables and on additional parameters that, in the case dealt with in this paper, are L_t, L_{pu}, r_t, r_{pu}, and R_L; they are considered as given values and do not vary during the optimization process. The reliability of the optimization method has been tested performing two runs of the optimization algorithm for each considered topology, assigning to the mutual inductance M, which acts as the sixth parameter of the objective functions, two extreme values. The largest one, denoted as M_{max}, is relevant to the condition of perfectly aligned coils while the lowest, equal to $M_{max}/4$ can be considered as the minimum M at which the induced voltage V_{pu} is enough to force the conduction of the diode rectifier and transfer power to the dc bus of the vehicle.

The actual implementation of the NSGA-II algorithm is designed to minimize the outputs of its objective functions and hence they have been defined as

$$f_1 = 1 - \eta \triangleq 1 - \frac{P_L}{P_s} \quad (1)$$

$$f_2 = \frac{1}{P_L} \quad (2)$$

where η is the power transfer efficiency, P_L is and the power transferred to R_L, and P_s is the active power delivered by the voltage source that supplies $\bar{V}_s$.

The procedure to compute both f_1 and f_2 starts working out the impedance $\dot{Z}_{pu}$ seen by the equivalent voltage source that represents the induced voltage $\bar{V}_{pu}$. It depends on the topology of CN_{pu} and on its actual set of design variables and parameters. Then, the reflected impedance $\dot{Z}_{ref}$ is computed. Its expression as a function of $\dot{Z}_{pu}$, given by (3), does not depend on the

topology nor on the variables or the parameters of the objective functions.

$$\dot{Z}_{ref} = \frac{\omega^2 M^2}{\dot{Z}_{pu}} \tag{3}$$

Then impedance $\dot{Z}_s$ is computed using the design variables and the parameters relevant to CN_t. The magnitude of $\bar{V}_s$ is conveniently set to 1, so that the reciprocal of $\dot{Z}_s$ corresponds to $\bar{I}_s$. From $\bar{I}_s$, $\bar{I}_t$ is computed solving the circuital equations of the network formed by CN_t, L_t, r_t and $\dot{Z}_{ref}$, and then the induced voltage $\bar{V}_{pu}$ is obtained as

$$\bar{V}_{pu} = -j\omega M \bar{I}_t \tag{4}$$

From the latter one, solving the circuital equation of CN_{pu}, $\bar{I}_L$ is obtained and finally P_L is computed in the form

$$P_L = \frac{1}{2} R_L |\bar{I}_L|^2 \tag{5}$$

where $|\bar{I}_L|^2$is the magnitude of $\bar{I}_L$.

From (5), f_2 is readily obtained according to (2). Before obtaining f_1, it is necessary to compute P_s as

$$P_s = \frac{1}{2} \Re e\left[\bar{V}_s \bar{I}_s^*\right] \tag{6}$$

where $\Re e[\cdot]$ is the operand that computes the real part of its argument, and then to substitute (5) and (6) in (1).

IV. SS COMPENSATION NETWORK OPTIMIZATION

The optimization algorithm has been at first applied to the CNs of a WPTS having the SS topology shown in Figure 2. The individuals are formed by only two design variables, i.e. X_t and X_{pu}, the impedances $\dot{Z}_{pu}$ and $\dot{Z}_s$ have the expressions

$$\dot{Z}_{pu} = R_L + jX_{pu} + r_{pu} + j\omega L_{pu} \tag{7}$$

$$\dot{Z}_s = jX_t + r_t + j\omega L_t + \dot{Z}_{ref} \tag{8}$$

and η and P_L are respectively

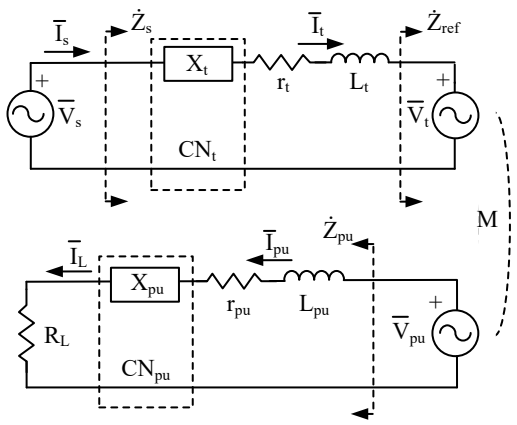

Figure 2. Circuital scheme of a WPTS with SS compensation networks.

TABLE I. WPTS PARAMETERS

Parameter	Symbol	Value
Track coil inductance	L_t	120 μH
Pickup coil inductance	L_{pu}	120 μH
Maximum mutual inductance	M_{max}	30 μH
Nominal load resistance	$R_{L,N}$	5.6 Ω
ESR of track coil	r_t	0.5 Ω
ESR of pickup	r_{pu}	0.5 Ω
Nominal supply angular frequency	ω_0	2π·85000

$$\eta = \frac{R_L \omega^2 M^2}{|\dot{Z}_{pu}|^2 \Re e[\dot{Z}_t] + \omega^2 M^2 \Re e[\dot{Z}_{pu}]} \tag{9}$$

$$P_L = \frac{1}{2} R_L \frac{\omega^2 M^2}{|\dot{Z}_t \dot{Z}_{pu} + \omega^2 M^2|^2} \tag{10}$$

where $\dot{Z}_t$, given by (11), is equal $\dot{Z}_s$ to without the contribute of $\dot{Z}_{ref}$.

$$\dot{Z}_t = jX_t + r_t + j\omega L_t \tag{11}$$

It is well known that efficiency is maximized when $X_{pu} = -\omega L_{pu}$ so that the term $|\dot{Z}_{pu}|^2 \Re e[\dot{Z}_t]$ in (9) is minimized [22]. The requirement of maximizing η does not impose any condition on X_t because the latter one does not affect $\Re e[\dot{Z}_t]$.

The optimization algorithm has been applied to populations made of 50 individuals. The individuals of the first generation have been extracted randomly in the range of [-500 Ω, 500 Ω]; for each of them and for each individual of the subsequent generations the corresponding quantities P_L and η have been computed using the parameters reported in Table I, which refer to a prototypal WPTS designed to charge the battery of a mini car [23]. The pairs (η, P_L) relevant to the initial generation of the first run of the algorithm, i.e. computed setting $M=M_{max}$ are plotted in Figure 3 using the magenta crosses.

In the first run, after 250 generations, the pairs (η, P_L) moved to the point marked by the blue diamonds in Figure 3. Analysis of the figure shows that the blue diamonds lay on a continuous line that constitutes the Pareto front. Each point of the front is

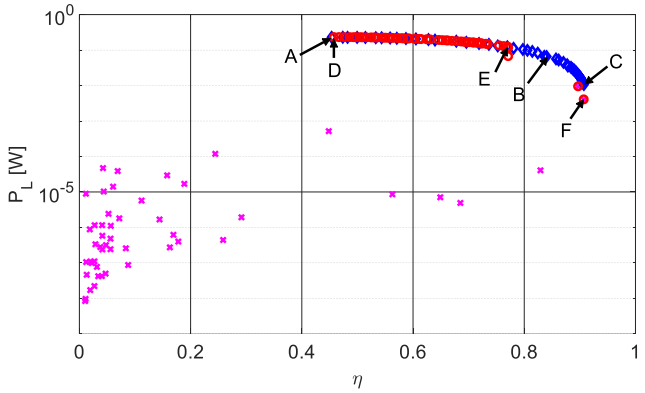

Figure 3. Pairs (η, P_L) relevant to the initial individuals (magenta crosses), to the final individuals with $M=M_{max}$ (blue diamonds), and to the final individuals with $M=M_{max}/4$ (red circles) for SS CNs.

TABLE II. OPTIMIZATION RESULTS WITH SS TOPOLOGY

	A	B	C	D	E	F
X_t [Ω]	-59.59	-79.83	-61.78	-65.12	-64.54	-118.69
X_{pu} [Ω]	-7.79	-79.89	-64.09	-76.61	-64.61	-64.07
η	0.4586	0.8402	0.9073	0.458	0.7705	0.9073
P_L [W]	0.2294	0.0659	0.0162	0.2295	0.1232	0.004

characterized by the property that it is not possible to change its corresponding design variables to obtain a better performance from one of the objective functions without worsen the performance of the other. This fact can be referred to the plot in Figure 3 stating that if a diamond moves on the right, i.e. toward higher efficiency, at the same time it must move down, i.e. toward lower power; or, conversely, that if a diamond moves upward, i.e. toward higher power, at the same time it must move on the left, i.e. toward lower efficiency.

Let us consider the two points at the extremities of the front and a third one chosen approximatively at the knee of the curve, where performance of the WPTS can be considered good both from the point of view of efficiency and of transferred power; they are denoted with A, B and C in Figure 3. Power, efficiency and design variables relevant to points A, B and C are reported in the leftmost columns of Table II. The listed values show that the algorithm somehow discovered that in order to obtain a high efficiency it is necessary to have a resonance at the pickup side of the WPTS; indeed, the resulting X_{pu} for point C is almost equal to the opposite of the reactance of L_t that, at the given supply frequency is 64Ω. In points A and B the transferred power is higher and, consequently efficiency is lower.

For the second run of the algorithm, the same initial individuals have been used, but the objective functions have been computed using $M=M_{max}/4$. The results obtained from the second run of the algorithm after 250 generations are marked by the red circles in Figure 3. It can be seen that most of the pairs (η, P_L) lay in the region characterized by lower efficiency of the same Pareto front obtained in the first run, with the exception of two points positioned in the rightmost end of the front. The results relevant to the three points denoted with D, E and F in Figure 3 are reported in rightmost columns of Table II.

Point D is at the beginning of the Pareto front obtained with $M=M_{max}/4$; it is nearly superimposed to A, but is obtained with quite different values of X_t and X_{pu}. Point E is the last of the sequence of red circles and corresponds to practically the same design variables as point C; however, it is characterized by lower efficiency and higher power. This result is easily explained considering that, for given $\dot{Z}_t$ and $\dot{Z}_{pu}$, expressions (9) and (10) are respectively and increasing and a decreasing function of M. Point F is one of the isolated point on the right. Curiously it corresponds with one of the starting points; probably its position has not been modified by the optimization algorithm because the corresponding X_{pu} already satisfy the condition of resonance and of efficiency maximization.

V. TT COMPENSATION TOPOLOGY OPTIMIZATION

After checking the algorithm on the simple SS compensation topology, it has been applied to optimize the much more complex CNs schematized in Figure 4. Both of them are formed by three

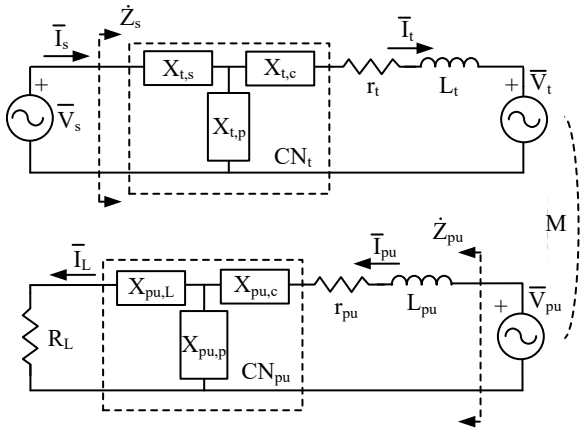

Figure 4. Circuital scheme of DWPTS with TT compensation networks.

elements arranged in a T connection and hence this topology is denoted as TT. Some works about TT topology have already been published but rather involved mathematical procedures were required because of the difficulties in approaching analytically its study [24].

Objective functions have been developed for the TT topology according to the procedure described in Section III.B and two runs of the optimization algorithm have been performed, also in this case setting M at first to M_{max} and then $M_{max}/4$ and using the same initial individuals for both the runs.

The pairs (η, P_L) relevant to the final individuals of the two runs are reported in Figure 5 following the same colors and symbols coding used in Figure 3. Also in this case it is possible to recognize two Pareto fronts to which the pairs (η, P_L) converge after 250 generations. As a comparison, the final pairs relevant to $M=M_{max}$ obtained with the SS topology are plotted as green crosses. From the figure it can be easily concluded that TT topology offers better performances than SS both from the point of view of efficiency and transferred power. This fact is confirmed by Tab. III, which reports optimization results obtained with the TT CNs. Also in this case, the pairs denoted as A and C at the ends of the Pareto together with the pair B laying on the knee of the front have been considered. Differently from what happened with SS topology, now the front has a sharp knee

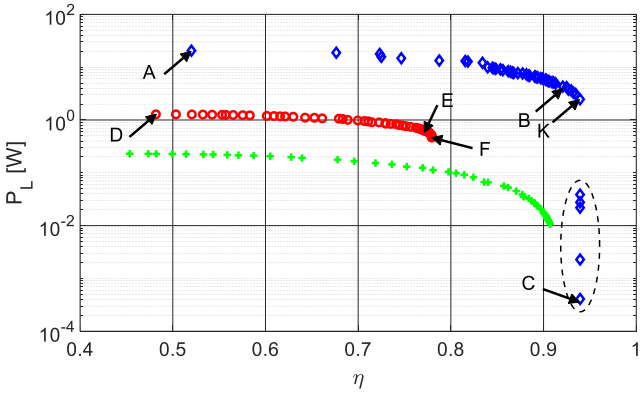

Figure 5. Pairs (η, P_L) relevant to the final individuals with $M=M_{max}$ (blue diamonds), and with $M=M_{max}/4$ (red circles) obtained with TT CNs. Pairs (η, P_L) relevant to the final individuals with $M=M_{max}$ obtained with SS topology (green stars).

TABLE III. OPTIMIZATION RESULTS WITH TT CNS

	A	B	C	D	E	F
$X_{t,s}$ [Ω]	-13.88	-13.87	-163.34	-151.66	-151.71	-153.27
$X_{t,p}$ [Ω]	-12.55	-12.56	-498.99	105.33	105.39	105.20
$X_{t,c}$ [Ω]	62.91	59.78	-87.02	-408.74	-409.22	-399.08
$X_{pu,c}$ [Ω]	-194.85	-192.56	230.74	-52.02	-57.52	-57.90
$X_{pu,p}$ [Ω]	-294.12	-144.44	235.99	14.68	-142.74	-40.19
$X_{pu,L}$ [Ω]	56.51	64.24	97.90	-11.54	-7.15	-6.62
η	0.520	0.921	0.939	0.482	0.7749	0.7796
P_L [W]	20.502	4.278	0.0004	1.270	0.5929	0.4608

that helps in selecting the pair B. Pairs D, E, and F have been selected on the Pareto front relevant to $M=M_{max}/4$ using the same criterions.

Analysis of Table III allows to recognize some interesting results. Points A and B, despite the large difference in the final values of the relevant pairs (η, P_L), differ sensibly only in reactance $X_{pu,p}$ and, marginally in $X_{pu,L}$ while $X_{pu,c}$ and the whole CN_t are nearly equal. The same considerations can be done also analyzing the reactances relevant to the pairs D, E and F so that it can be hypothesized that $X_{pu,c}$ and the reactances of CN_t element depend only on M, while $X_{pu,L}$ and $X_{pu,c}$ change considering different pairs on a given Pareto front.

The table shows that the reactances relevant to the pair C are completely different from those corresponding to A and B and that $X_{t,p}$ is very near to the boundary of its allowed range of variation, indicating that probably better performance could be reached with a further increase of the magnitude of this this reactance or even with its disconnection from the circuit. The other four pairs laying in the vertical branch of the Pareto front and enclosed by the dashed ellipse are obtained using the same CN_{pu} and $X_{t,c}$ as pair C, but different $X_{t,p}$, which is still high but does not reach the boundary of the allowed interval; their relevant $X_{t,s}$ is also different from that of pair C and is positive for three of these pairs and negative for one of them.

Characteristics of pair C are rather peculiar and in the next Section it will be shown that adoption of the corresponding CNs does not guarantee a satisfactory functioning of the DWPTS.

It is worth to notice that none of the individuals relevant to the pairs outside the ellipse and none of the individuals selected with $M=M_{max}/4$ has design variables near to zero or to the boundary of the allowed variation range. This fact means that all the elements of the CNs contribute to obtaining the reported performance and does not need to be shorted of disconnected from the circuits.

VI. RESULTS VALIDATION

Usually CNs functioning is based on some kind of resonance between their elements. Resonance is enforced because it generally helps in reducing the required supply voltage and/or the coils currents and makes nearly sinusoidal most of the voltages and currents involved in the WPTSs functioning, thus reducing the losses inherent to higher order harmonics and increasing the system efficiency.

The objective functions used in this paper consider a purely sinusoidal waveform for the currents even if it is well known that

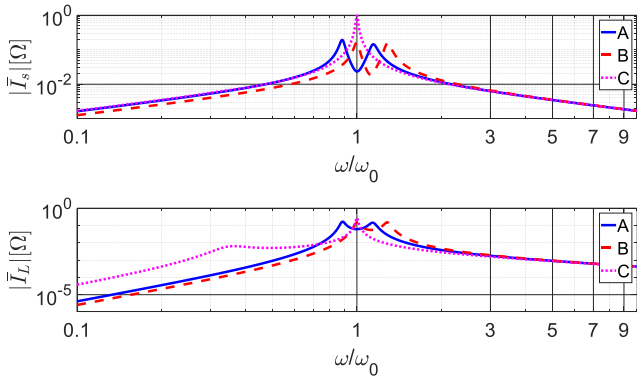

Figure 6. Bode diagrams of $\bar{I}_s$ and $\bar{I}_L$ obtained with SS topology using the design variables relevant to the pairs A, B and C of Table II.

actually the supply voltage has a square waveform. For this reason, the selected CNs achieve the computed performance only if they exert some sort of filtering effect on the electric quantities. Being the objective functions aimed at maximizing the efficiency and the transferred power, the harmonic contents reduction is mostly required on the currents $\bar{I}_s$ and $\bar{I}_L$.

Existence and effectiveness of filtering effect have been checked computing the magnitude Bode diagram of the two currents considering the CNs having the design variables relevant to the pairs A, B and C. The diagrams relevant to SS topology are reported in Figure 6 while those related to TT topology are shown in Figure 7. In both the figures, the blue solid lines denote pairs A, the red dashed line denote points B and the dotted magenta lines denote points C; moreover, the supply angular frequency has been normalized with respect to the nominal one. Analysis of Figure 6 shows that all the three sets of design variables enforce a resonance at the nominal supply frequency in both the CN_t and the CN_{pu}, even if the resonances are not all of the same type. In any case, higher order harmonics of the currents are effectively attenuated by the CNs actions.

The same conclusions can be drawn also for the TT topology, except for the CNs relevant to pair C: in this case, no resonance happens at $\omega=\omega_0$ and the filtering effect is rather poor both at the transmitting coil and at the pickup side. As a comparison, the Bode diagrams obtained considering the design variable relevant to pair K of Figure 5 is plotted with the black line. It is practically superimposed to the diagrams obtained from the CNs relevant to the pairs A and B despite pair K lays on the opposite end of the

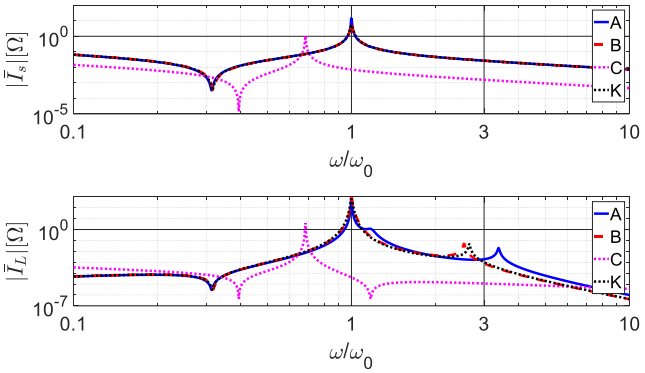

Figure 7. Bode diagrams of $\bar{I}_s$ and $\bar{I}_L$ obtained with TT topology using the design variables relevant to the pairs A, B, C of Table III, and K of Figure 5.

Pareto front with respect to pair A. From comparison of figures 6 and 7 it results that with TT topology the CNs are even more effective than those of SS topology in filtering the current harmonics, thus validating the results obtained in Section V.

VII. Conclusions

The paper presented an approach to the design of the CNs of the WPTSs that is alternative to the circuital analysis dealt with in most of the works related to this topic. The use of a genetic optimization algorithm allows to study exhaustively the performance of CNs having complex topology and that could not be easily analyzed following the conventional approach based on the circuital equations. The optimization algorithm has been at first checked on the well known SS topology and resulted able to converge to the reactances that optimize the efficiency and the transferred power. Then the algorithm has been applied to CNs having the TT topology. Also in this case it was able to recognize a number of optimal sets of design variables that give origin to new compensation topologies characterized by even better performance in terms of efficiency and transferred power.

In both cases the algorithm demonstrates its ability to operate correctly with two much different values of the mutual inductance, thus suggesting that it could be adapted to the design of the CNs of dynamic WPTSs.

In the case of TT topology, it resulted necessary to check the compliance of the obtained CNs with the hypothesis of operating with sinusoidal currents, used in computing the objective functions, because at least one of the proposed solutions leads to distorted currents in the coils.

References

[1] S. Y. Choi, B. W. Gu, S. Y. Jeong, and C. T. Rim, "Advances in Wireless Power Transfer Systems for Roadway-Powered Electric Vehicles," *IEEE Journal of Emerging and Selected Topics in Power Electronics*, vol. 3, no. 1, pp. 18–36, Mar. 2015.

[2] G. A. Covic and J. T. Boys, "Inductive power transfer," *Proceedings of the IEEE*, vol. 101, no. 6, pp. 1276–1289, 2013.

[3] H. Feng, T. Cai, S. Duan, X. Zhang, H. Hu, and J. Niu, "A Dual-Side-Detuned Series–Series Compensated Resonant Converter for Wide Charging Region in a Wireless Power Transfer System," *IEEE Transactions on Industrial Electronics*, vol. 65, no. 3, pp. 2177–2188, Mar. 2018.

[4] J. L. Villa, J. Sallan, J. F. Sanz Osorio, and A. Llombart, "High-Misalignment Tolerant Compensation Topology For ICPT Systems," *IEEE Transactions on Industrial Electronics*, vol. 59, no. 2, pp. 945–951, Feb. 2012.

[5] P. Di Barba, M. E. Mognaschi, D. A. Lowther, and J. K. Sykulski, "A Benchmark TEAM Problem for Multi-Objective Pareto Optimization of Electromagnetic Devices," *IEEE Transactions on Magnetics*, vol. 54, no. 3, pp. 1–4, Mar. 2018.

[6] Di Barba, P., M. E. Mognaschi, D. A. Lowther, and S. Wiak, "Field-based optimal-design of an electric motor: a new sensitivity formulation," *Open Physics*, vol. 15, no. 1, pp. 924–928, Dec. 2017.

[7] E. Zitzler, L. Thiele, M. Laumanns, C. M. Fonseca, and V. G. da Fonseca, "Performance assessment of multiobjective optimizers: an analysis and review," *IEEE Transactions on Evolutionary Computation*, vol. 7, no. 2, pp. 117–132, Apr. 2003.

[8] E. Zitzler and L. Thiele, "Multiobjective evolutionary algorithms: a comparative case study and the strength Pareto approach," *IEEE Transactions on Evolutionary Computation,* vol. 3, no. 4, pp. 257–271, 1999.

[9] N. Srinivas and K. Deb, "Multiobjective optimization using nondominated sorting in genetic algorithms," *Evolutionary Computation*, vol. 2, pp. 221–248, 1994.

[10] P. Di Barba, M. E. Mognaschi, S. Wiak, M. Przybylski, and B. Slusarek, "Optimization and measurements of switched reluctance motors exploiting soft magnetic composite," *International Journal of Applied Electromagnetics and Mechanics*, vol. 57, pp. 83–93, Apr. 2018.

[11] P. Di Barba, M. E. Mognaschi, M. Przybylski, N. Rezaei, B. Slusarek, and S. Wiak, "Geometry optimization for a class of switched-reluctance motors: A bi-objective approach," *International Journal of Applied Electromagnetics and Mechanics*, vol. 56, pp. 107–122, Feb. 2018.

[12] P. Di Barba, B. Liu, M. E. Mognaschi, P. Venini, and S. Wiak, "Multiphysics field analysis and evolutionary optimization: Design of an electro-thermo-elastic microactuator," *International Journal of Applied Electromagnetics and Mechanics*, vol. 54, no. 3, pp. 433–448, Jul. 2017.

[13] E. Costamagna, P. Di Barba, M. E. Mognaschi, and A. Savini, "Fast Algorithms for the Design of Complex-Shape Devices in Electromechanics," in *Computational Methods for the Innovative Design of Electrical Devices*, vol. 327, S. Wiak and E. Napieralska-Juszczak, Eds. Berlin, Heidelberg: Springer Berlin Heidelberg, 2010, pp. 59–86.

[14] S. Carcangiu, P. Di Barba, A. Fanni, M. E. Mognaschi, and A. Montisci, "Comparison of multi-objective optimisation approaches for inverse magnetostatic problems," *COMPEL - The international journal for computation and mathematics in electrical and electronic engineering*, vol. 26, no. 2, pp. 293–305, Apr. 2007.

[15] Ziyan Ren, Minh-Trien Pham, and Chang Seop Koh, "Robust Global Optimization of Electromagnetic Devices With Uncertain Design Parameters: Comparison of the Worst Case Optimization Methods and Multiobjective Optimization Approach Using Gradient Index," *Magnetics, IEEE Transactions on*, vol. 49, no. 2, pp. 851–859, Feb. 2013.

[16] P. Di Barba, M. E. Mognaschi, R. Palka, P. Paplicki, and S. Szkolny, "Design optimization of a permanent-magnet excited synchronous machine for electrical automobiles," *International Journal of Applied Electromagnetics and Mechanics*, vol. 39, no. 1–4, pp. 889–895, 2012.

[17] P. Di Barba, F. Dughiero, M. E. Mognaschi, A. Savini, and S. Wiak, "Biogeography-Inspired Multiobjective Optimization and MEMS Design," *IEEE Transactions on Magnetics*, vol. 52, no. 3, pp. 1–4, Mar. 2016.

[18] P. Di Barba, M. E. Mognaschi, A. Savini, and S. Wiak, "Island biogeography as a paradigm for MEMS optimal design," *International Journal of Applied Electromagnetics and Mechanics*, vol. 51, no. s1, pp. S97–S105, Apr. 2016.

[19] Di Barba P., F. Dughiero, M. Forzan, M. E. Mognaschi, and Sieni E., "New solutions to a multi-objective benchmark problem of induction heating: an application of computational biogeography and evolutionary algorithms," *Archives of Electrical Engineering*, vol. 67, no. 1, pp. 139–149, 2018.

[20] P. Di Barba, L. Fassina, G. Magenes, and M. E. Mognaschi, "Shape synthesis of a well-plate for electromagnetic stimulation of cells," *International Journal of Numerical Modelling: Electronic Networks, Devices and Fields*, p. e2259, Jun. 2017.

[21] K. Deb, A. Pratap, S. Agarwal, and T. Meyarivan, "A fast and elitist multiobjective genetic algorithm: NSGA-II," *IEEE Transactions on Evolutionary Computation, v*ol. 6, no. 2, pp. 182–197, 2002.

[22] M. K. Naik, M. Bertoluzzo, and G. Buja, "Design of a contactless battery charging system," in *2013 Africon*, 2013, pp. 1–6.

[23] G. Buja, M. Bertoluzzo, and K. N. Mude, "Design and Experimentation of WPT Charger for Electric City Car," *IEEE Transactions on Industrial Electronics*, vol. 62, no. 12, pp. 7436–7447, Dec. 2015.

[24] X. Qu, Y. Jing, H. Han, S. C. Wong, and C. K. Tse, "Higher Order Compensation for Inductive-Power-Transfer Converters With Constant-Voltage or Constant-Current Output Combating Transformer Parameter Constraints," *IEEE Transactions on Power Electronics*, vol. 32, no. 1, pp. 394–405, Jan. 2017.